

Surface Catalysis of Water Oxidation by the Blue Ruthenium Dimer

Jonah W. Jurss, Javier C. Concepcion, Michael R. Norris, Joseph L. Templeton, and Thomas J. Meyer*

Department of Chemistry, University of North Carolina at Chapel Hill, Chapel Hill, North Carolina 27599

Received March 10, 2010

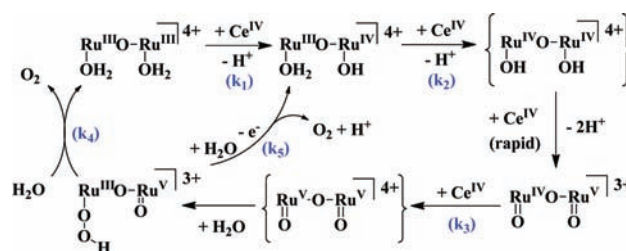
Single-electron activation of multielectron catalysis has been shown to be viable in catalytic water oxidation with stepwise proton-coupled electron transfer, leading to high-energy catalytic precursors. For the blue dimer, *cis,cis*-[(bpy)₂(H₂O)Ru^{III}ORu^{III}(H₂O)(bpy)₂]⁴⁺, the first well-defined molecular catalyst for water oxidation, stepwise 4e⁻/4H⁺ oxidation occurs to give the reactive precursor [(O)Ru^VORu^V(O)]⁴⁺. This key intermediate is kinetically inaccessible at an unmodified metal oxide surface, where the only available redox pathway is electron transfer. We report here a remarkable surface activation of indium–tin oxide (In₂O₃:Sn) electrodes toward catalytic water oxidation by the blue dimer at electrodes derivatized by surface phosphonate binding of [Ru(4,4'-((HO)₂P(O)CH₂)₂bpy)₂]²⁺. Surface binding dramatically improves the rate of surface oxidation of the blue dimer and induces water oxidation catalysis.

The multielectron nature of water oxidation, 2H₂O → O₂ + 4e⁻ + 4H⁺, poses significant mechanistic challenges. For example, mechanisms involving 1e⁻ oxidation and hydroxyl radical as an intermediate with E°(*OH/H₂O) = 2.8 V vs NHE are too slow to be of interest, which can be significantly inhibiting at electrode surfaces where the only available pathway is electron transfer.¹

In an earlier study, we reported that Ce^{IV} water oxidation, catalyzed by the blue ruthenium dimer *cis,cis*-[(bpy)₂(H₂O)Ru^{III}ORu^{III}(OH₂)(bpy)₂]⁴⁺ {[(H₂O)Ru^{III}ORu^{III}(OH₂)]⁴⁺}, can be enhanced by factors of up to 30 with added electron-transfer mediators such as [Ru(bpy)₃]²⁺ (bpy = 2,2'-bipyridine). The rate enhancement was due to slow intrinsic electron transfer by the Ce^{IV}/III couple and rapid electron transfer by the mediator.² In this manuscript, we report a pronounced surface activation effect at Sn^{IV}-doped In₂O₃ (ITO, indium–tin oxide) electrodes modified by surface binding of a functionalized [Ru(bpy)₃]²⁺ complex.

The mechanism of water oxidation in solutions dilute in blue dimer with Ce^{IV} as oxidant, in catalytic excess, is shown in Scheme 1. It features oxidation to a transient intermediate [(O)Ru^VORu^V(O)]⁴⁺, which undergoes a rapid reaction with water to give a transiently stable peroxidic intermediate. In

Scheme 1. Mechanism of Ce^{IV}-Catalyzed Water Oxidation by the Blue Dimer at pH 1: $k_1 = 630 \text{ M}^{-1} \text{ s}^{-1}$, $k_2 = 3.2 \text{ M}^{-1} \text{ s}^{-1}$, $k_3 = 2.0 \times 10^2 \text{ M}^{-1} \text{ s}^{-1}$, and $k_4 = 2 \times 10^{-3} \text{ s}^{-1}$ (Measured in 0.1 M HClO₄) at 23 ± 2 °C



0.1 M HClO₄, the latter decomposes by first-order kinetics and evolves oxygen (k_4 in Scheme 1).³

In cyclic voltammograms (CVs) of the blue dimer in 0.1 M triflic acid (HOTf), an electrochemically reversible, scan rate dependent, 1e⁻ wave appears at $E_{1/2} = 1.04 \text{ V}$ vs NHE for the [(H₂O)Ru^{III}ORu^{IV}(OH)]⁴⁺/[(H₂O)Ru^{III}ORu^{III}(OH₂)]⁴⁺ couple (Figure 1A). A dramatically different response (Figure 1B) appears at ITO electrodes with chemically linked, phosphonate-derivatized [Ru(4,4'-((HO)₂P(O)CH₂)₂bpy)₂-(bpy)]²⁺ [ITO-Ru²⁺; 4,4'-((HO)₂P(O)CH₂)₂bpy = 4,4'-bis-(methyl)phosphonato-2,2'-bipyridine].⁴

Synthesis and characterization of the complex is described in Supporting Information (SI). It was added to ITO by soaking the electrodes for extended periods in methanol solutions containing the complex (Figure SI1 in the SI). Surface coverages (Γ in mol cm⁻²) were determined by integration of the cathodic peak area for the surface Ru^{III/II} wave at $E_{1/2} = 1.31 \text{ V}$ vs NHE at pH 1 (Figure 1A) after background subtraction and conversion of coulombs to mol cm⁻² as described previously.⁵ Maximum coverages of $\Gamma \sim 1 \times 10^{-10} \text{ mol cm}^{-2}$ were obtained. Peak currents (i_p) for the surface

(3) Liu, F.; Concepcion, J. J.; Jurss, J. W.; Cardolaccia, T.; Templeton, J. L.; Meyer, T. J. *Inorg. Chem.* 2008, 47, 1727–1752. See Supporting Information, page S13, for additional comments regarding the rate constants shown in Scheme 1.

(4) (a) Utilization of a previously published synthetic procedure for the surface catalyst, [Ru(4,4'-((HO)₂P(O)CH₂)₂bpy)₂](bpy)Cl₂·4b gave CV surface enhancements but with qualitatively different waveforms (Figures SI12–SI14 in the SI). As will be discussed in a later manuscript, these preparations gave greater than monolayer coverages and the products appear to be oligomeric in nature. (b) Will, G.; Boschloo, G.; Rao, S. N.; Fitzmaurice, D. J. *Phys. Chem. B* 1999, 103(38), 8067–8079.

(5) Meyer, T. J.; Meyer, G. J.; Pfennig, B. W.; Schoonover, J. R.; Timpson, C. J.; Wall, J. F.; Kobusch, C.; Chen, X.; Peek, B. M.; Wall, C. G.; Ou, W.; Erickson, B. W.; Bignozzi, C. A. *Inorg. Chem.* 1994, 33, 3952–3964.

*To whom correspondence should be addressed. E-mail: tjmeyer@email.unc.edu.

(1) Costentin, C.; Robert, M.; Savéant, J.-M. *J. Electroanal. Chem.* 2006, 588, 197–206.

(2) Concepcion, J. J.; Jurss, J. W.; Templeton, J. L.; Meyer, T. J. *Proc. Natl. Acad. Sci. U.S.A.* 2008, 105(46), 17632–17635.

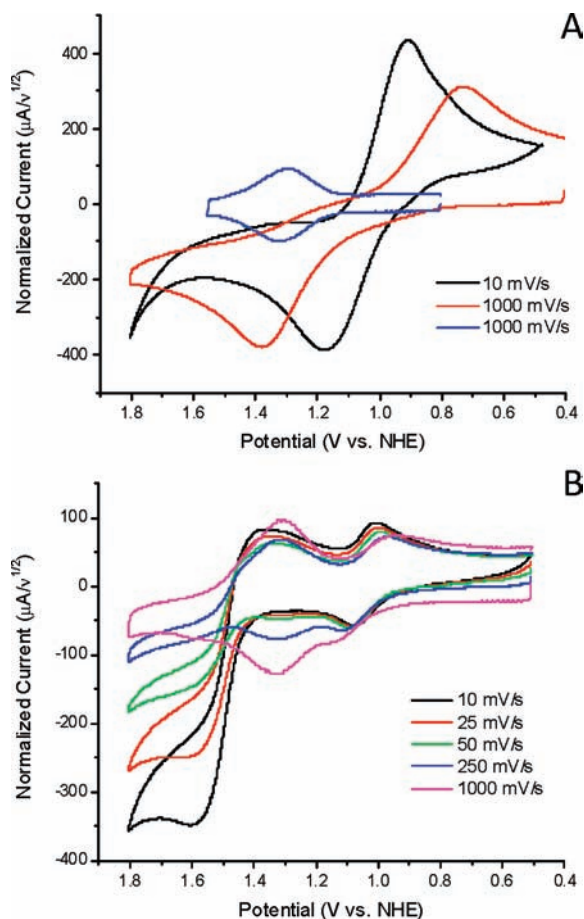


Figure 1. (A) Scan rate normalized ($i_p/v^{1/2}$) CVs of 1 mM blue dimer in 0.1 M HOTf at an ITO electrode (1.55 cm^2) at scan rates of 10 and 1000 mV s^{-1} and at $23 \pm 2 \text{ }^\circ\text{C}$. A CV (i_p/v) of surface-adsorbed $[\text{Ru}(4,4'-(\text{HO})_2\text{P}(\text{O})\text{CH}_2)_2\text{bpy})_2(\text{bpy})]^{2+}$ on ITO (ITO-Ru^{2+} , $\Gamma = 1.0 \times 10^{-10} \text{ mol cm}^{-2}$, 1.55 cm^2) is shown in blue. (B) CVs ($i_p/v^{1/2}$) of $1.0 \times 10^{-4} \text{ M}$ blue dimer in 0.1 M HOTf at ITO-Ru^{2+} ($\Gamma = 1.0 \times 10^{-10} \text{ mol cm}^{-2}$, 1.5 cm^2) at various scan rates.

$\text{Ru}^{\text{III/II}}$ wave vary linearly with the scan rate (v), as expected for a surface-confined couple (Figures SI2 and SI3 in the SI).⁶

At the modified electrode with added blue dimer, the $[(\text{H}_2\text{O})\text{Ru}^{\text{III}}\text{ORu}^{\text{IV}}(\text{OH})]^{4+}/[(\text{H}_2\text{O})\text{Ru}^{\text{III}}\text{ORu}^{\text{III}}(\text{OH}_2)]^{4+}$ wave appears at $E_{1/2} = 1.04 \text{ V}$ and an additional oxidative wave at $E_{p,a} = 1.57 \text{ V}$ for the $3e^-/3\text{H}^+$ couple,⁷ $[(\text{H}_2\text{O})\text{Ru}^{\text{III}}\text{ORu}^{\text{IV}}(\text{OH})]^{4+} \xrightarrow{-3e^-, -3\text{H}^+} [(\text{O})\text{Ru}^{\text{V}}\text{ORu}^{\text{V}}(\text{O})]^{4+}$. Peak currents for both waves vary with $v^{1/2}$, consistent with diffusional couples (Figures SI4 and SI5 in the SI).⁶

The dramatic current enhancement for the $3e^-/3\text{H}^+$ wave at 1.57 V is due to an enhancement of the rate-limiting electron-transfer oxidation of $[(\text{H}_2\text{O})\text{Ru}^{\text{III}}\text{ORu}^{\text{IV}}(\text{OH})]^{4+}$ to $\text{Ru}^{\text{IV}}\text{ORu}^{\text{IV}}$ (presumably as $[(\text{HO})\text{Ru}^{\text{IV}}\text{ORu}^{\text{IV}}(\text{OH})]^{4+}$ at this pH,⁸ eq 1a). $\text{Ru}^{\text{IV}}\text{ORu}^{\text{IV}}$ is a kinetic intermediate unstable toward disproportionation with $E^\circ(\text{Ru}^{\text{IV}}\text{ORu}^{\text{IV}}/\text{Ru}^{\text{IV}}\text{ORu}^{\text{III}}) > E^\circ(\text{Ru}^{\text{V}}\text{ORu}^{\text{IV}}/\text{Ru}^{\text{IV}}\text{ORu}^{\text{IV}})$.^{3,8} Once formed in the rate-limiting step, it undergoes further $2e^-/2\text{H}^+$ oxidation

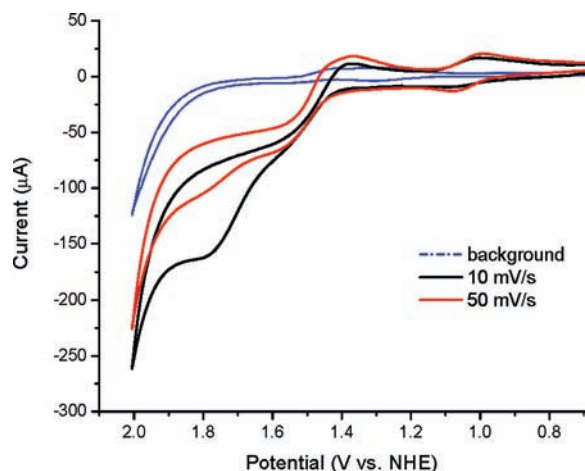
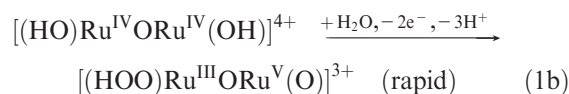
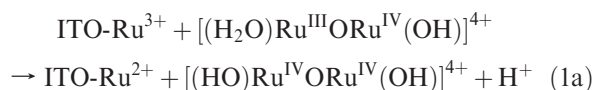
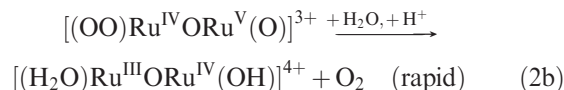
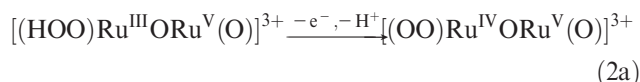


Figure 2. CVs of the peroxido intermediate formed by addition of $3 \times 10^{-4} \text{ M}$ Ce^{IV} to $1.0 \times 10^{-4} \text{ M}$ $[(\text{H}_2\text{O})\text{Ru}^{\text{III}}\text{ORu}^{\text{IV}}(\text{OH})]^{4+}$ in 0.1 M HOTf with surface-adsorbed $[\text{Ru}(4,4'-(\text{HO}_2)_2\text{P}(\text{O})\text{CH}_2)_2\text{bpy})_2(\text{bpy})]^{2+}$ on ITO ($\Gamma = 1.0 \times 10^{-10} \text{ mol cm}^{-2}$; 1.52 cm^2). The background is of $3.0 \times 10^{-4} \text{ M}$ Ce^{III} in 0.1 M HOTf at the same electrode.

to $[(\text{O})\text{Ru}^{\text{V}}\text{ORu}^{\text{V}}(\text{O})]^{4+}$, followed by water attack to give the peroxide (eq 1b).



A mechanism related to Scheme 1 also holds for the surface-mediated reaction. At even higher potentials, a catalytic water oxidation wave appears with an onset at $\sim 1.7 \text{ V}$. Catalytic water oxidation at these potentials appears to be triggered by further oxidation of the peroxidic intermediate $[(\text{HOO})\text{Ru}^{\text{III}}\text{ORu}^{\text{V}}(\text{O})]^{3+}$ to $[(\text{OO})\text{Ru}^{\text{IV}}\text{ORu}^{\text{V}}(\text{O})]^{3+}$ (k_5 in Scheme 1) followed by rapid oxygen release (eq 2). In CVs of this intermediate {generated by the addition of $3 \times \text{Ce}^{\text{IV}}$ to $[(\text{H}_2\text{O})\text{Ru}^{\text{III}}\text{ORu}^{\text{IV}}(\text{OH})]^{4+}$ } at a mediator-modified electrode (Figure 2), an irreversible oxidation wave appears at $\sim 1.8 \text{ V}$ on a catalytic background. The peroxidic intermediate is further characterized by $\lambda_{\text{max}} = 482 \text{ nm}$ ($\epsilon = 13\,200 \text{ M}^{-1} \text{ cm}^{-1}$)³ and a wave for a $(\text{HOO})\text{Ru}^{\text{III}}\text{ORu}^{\text{V}}/(\text{HOO})\text{Ru}^{\text{III}}\text{ORu}^{\text{IV}}$ couple at $E_{1/2} = 1.03 \text{ V vs NHE}$.



As noted below, holding the potential past E° for the $\text{Ru}^{\text{III/II}}$ wave at 1.31 V leads to electrocatalytic water oxidation. Peak currents increase linearly with surface coverage of the mediator and with concentration of the blue dimer in the external solution (Figures SI6 and SI7 in the SI). The rate constant for surface oxidation of the blue dimer calculated from catalytic current measurements (Figure SI6 in the SI) is $k_{\text{cat}} = 2.1 \times 10^3 \text{ M}^{-1} \text{ s}^{-1}$. Catalysis is not observed at bare

(6) Bard, A. J.; Faulkner, L. R. *Electrochemical Methods. Fundamentals and Applications*, 2nd ed.; John Wiley & Sons, Inc.: New York, 2001.

(7) Gilbert, J. A.; Eggleston, D. S.; Murphy, W. R., Jr.; Geselowitz, D. A.; Gersten, S. W.; Hodgson, D. J.; Meyer, T. J. *J. Am. Chem. Soc.* **1985**, *107*, 3855–3864.

(8) Bartolotti, L. J.; Pedersen, L. G.; Meyer, T. J. *Int. J. Quantum Chem.* **2001**, *83*, 143–149.

ITO electrodes. In our earlier report, a comparable rate enhancement of blue dimer catalysis was observed with $k_{\text{cat}} = 1.9 \times 10^3 \text{ M}^{-1} \text{ s}^{-1}$ for $[\text{Ru}(\text{bpy})_3]^{2+}$ as the mediator in solution.²

A complication appears in CV data at higher blue dimer concentrations, especially in HClO_4 , arising from the adsorption/microprecipitation of salts of $[(\text{O})\text{Ru}^{\text{V}}\text{ORu}^{\text{V}}(\text{O})]^{4+}$ on the electrode surface. Adsorption is characterized by a reductive spike in the current–potential profile at $E_{\text{p,c}} = 1.43 \text{ V}$ in reverse scans (Figures SI8 and SI9 in the SI). Under other conditions, a nearly reversible $3\text{e}^-/3\text{H}^+$ surface wave is observed (Figure SI10 in the SI).⁷ A related effect has been reported for chemical oxidation of the blue dimer with $\times 4 \text{ Ce}^{\text{IV}}$ in ice cold 1.0 M HClO_4 .^{9,10}

Depending on the solution conditions, blue dimer adsorption causes a slow loss of surface catalysis over time as the mediator is lost from the surface. Steady-state surface loading was maintained by adding $2.5 \times 10^{-5} \text{ M}$ $[\text{Ru}(4,4'-((\text{HO}_2)_2\text{-P}(\text{O})\text{CH}_2)_2\text{bpy})_2(\text{bpy})]^{2+}$ to the external solution to maintain a monolayer surface coverage (Figure SI1 in the SI).

Electrocatalytic water oxidation was investigated with 0.5 mM blue dimer in the external solution in 0.1 M HOTf at an applied potential of 1.46 V vs NHE, just past the $\text{Ru}^{\text{III/II}}$ surface couple at 1.31 V (Figure SI11 in the SI). Steady-state, catalytic current densities of $44 \mu\text{A cm}^{-2}$ were obtained for more than 5 h under these conditions. At this potential, water oxidation is initiated by oxidation of the mediator with an overvoltage of $\sim 0.3 \text{ V}$ relative to the $\text{O}_2/\text{H}_2\text{O}$ couple. Illustrating the importance of catalyst surface binding, there was no evidence for catalysis at an unmodified ITO electrode with $2.5 \times 10^{-5} \text{ M}$ $[\text{Ru}(\text{bpy})_3]^{2+}$ in the external solution.

Evolved oxygen measurements in an airtight electrochemical cell confirmed the electrocatalytic production of oxygen. O_2 was measured by the difference in the initial reading of O_2 in the headspace of an airtight, degassed electrochemi-

cal cell and the final reading. The final reading was stable indefinitely. After 500 min of electrolysis at 1.46 V , 0.95 C had passed, producing $2.5 \times 10^{-6} \text{ mol}$ of O_2 , corresponding to 17 500 turnovers of the surface mediator, 1.25 turnovers of the blue dimer, and a Faradaic efficiency of 95%.

Spectrophotometric monitoring revealed that the dominant form of the catalyst in the initial stages of the electrolysis was $[(\text{H}_2\text{O})\text{Ru}^{\text{III}}\text{ORu}^{\text{IV}}(\text{OH})]^{4+}$ ($\lambda_{\text{max}} = 495 \text{ nm}$; $\epsilon = 22\,000 \text{ M}^{-1} \text{ cm}^{-1}$), consistent with its rate-limiting oxidation to $\text{Ru}^{\text{IV}}\text{ORu}^{\text{IV}}$. As the electrolysis proceeds, the spectrum shifts to 492 nm , consistent with earlier observations of anation to form $[(\text{H}_2\text{O})\text{Ru}^{\text{III}}\text{ORu}^{\text{IV}}(\text{OTf})]^{4+}$.³ Anated intermediates inhibit catalysis because of the requirement to undergo aquation before re-entering the catalytic cycle.

Our results demonstrate that multielectron-transfer water oxidation catalysis can be accelerated by mediating interfacial electron transfer near the potential of the $\text{O}_2/\text{H}_2\text{O}$ couple with relatively low overvoltages. There are potentially important implications for photodriven water oxidation as well.¹¹

Acknowledgment. Funding by the Chemical Sciences, Geosciences and Biosciences Division of the Office of Basic Energy Sciences, U.S. Department of Energy (Grant DE-FG02-06ER15788) and UNC EFRC: Solar Fuels and Next Generation Photovoltaics, an Energy Frontier Research Center funded by the U.S. Department of Energy, Office of Science, Office of Basic Energy Sciences (Award No. DE-SC0001011) is gratefully acknowledged. J.W.J. thanks the Graduate Assistance in Areas of National Need Program for a fellowship.

Supporting Information Available: Detailed synthetic procedures, electrode preparation and instrumentation, surface loading isotherms, and electrochemical results. This material is available free of charge via the Internet at <http://pubs.acs.org>.

(9) Binstead, R. A.; Chronister, C. W.; Ni, J.; Hartshorn, C. M.; Meyer, T. J. *J. Am. Chem. Soc.* **2000**, *122*, 8464–8473.

(10) Cape, J. L.; Lyman, S. V.; Lightbody, T.; Hurst, J. K. *Inorg. Chem.* **2009**, *48*, 4400–4410.

(11) Concepcion, J. J.; Jurss, J. W.; Hoertz, P. G.; Meyer, T. J. *Angew. Chem., Int. Ed.* **2009**, *48*, 9473–9476.